Journal of Mechanical Research and Application (JMRA), Vol. 12 No.1, 1400(2021),33-42

Influence of N_2/Ar flow ratio on the structural, mechanical properties and corrosion behavior of TaN films

M. Manouchehrian

Department of Physics, South Tehran Branch, Islamic Azad University, Tehran, Iran

Abstract

TaN films with different N_2/Ar flow ratios were deposited on 304 stainless steel using the magnetron sputtering method. The effect of N_2/Ar flow ratios on the mechanical properties, corrosion behavior, morphology and phase structure of the films are investigated by X-ray diffraction (XRD), atomic force microscopy (AFM), nanoindentation and corrosion mechanism study. The XRD results confirmed that increasing N_2/Ar flow ratio does not affect the formation of the new phases but intensity of peaks increased. AFM images showed that surface roughness and grain size increased with increasing of N_2/Ar flow ratio. It was found that hardness decreased as N_2/Ar flow ratio increased. The potentiodynamic polarization was carried out in 0.5 M NaCl solution to study the corrosion of films. From the corrosion test it can be inferred that the amount of N_2/Ar flow ratio plays an important role for reducing the corrosion.

Keywords : Tantalum, hardness, AFM, XRD, corrosion

1 Introduction

Transition metal nitride films, such as CrN, TiN, TaN, etc., have been utilized for cutting and drilling tools due to their excellent hardness, wear, and corrosion resistance [1-4]. TaN films are used in a wide variety of applications such as thin film resistors, diffusion barriers in microelectronic [5-9], and surface protective coatings as well as [10,11]. There are valuable investigation on the mechanical properties and thermal stability of TaN films, indicating its potential application as hard coatings [10,11]. However, the overall published reports for TaN are for less than other nitrides, such as TiN and CrN. In the physical vapor deposition, PVD, TaN films shows a variety of compound solutions, including BCC α-TaN, hexagonal γ TaN, Ta_2N, WC structure, cubic NaCl TaN, tetragonal Ta_4N_5 and orthorombic Ta_3N_5 [12,13]. The structures of TaN films prepared by PVD method depend intimately on the deposition technique and the process parameters. Multilayer structure and related mechanical and corrosion behavior were also intensively studied [14]. In this work, we propose to study the effect of N_2 partial pressure in TaN films into consideration the microstructure, surface morphology, mechanical properties and corrosion behavior of the films.

2 Experimental Details

The tantalum nitride films with thickness of 800 nm measured by quartz microbalance, were deposited on 304 stainless steel by magnetron sputtering technique. The target diameter and thickness were 50 mm and 6 mm and distance of target to substrate is 100 mm. The substrates were cut into 10 mm×10 mm slabs then they were cleaned with acetone and ethanol in an ultrasonic bath for 30 min. The vacuum chamber base pressure was 2×10^{-5} mbar. Argon (99.999%) and nitrogen (99.999%) were introduced

into the chamber through mass flow controllers, which were used as the sputtering and reactive gases, respectively. During the deposition the bias voltage and substrates temperature were fixed at -220 V and 300 K respectively. Prior to deposition, substrates were bombarded by argon ions produced in electric discharge chamber for 30 min. The TaN were deposited on 304 stainless steel with different N_2/Ar flow ratios which is summarised in Table 1. Deposition rate was estimated to be 10 nm/min. The phase and crystalline structure of the films were characterized by X-ray diffraction (XRD) using a Philips-pw 1800 with Cu(K_α) radiation (λ=0.15406) which was operated at 40 kV and 30 mA. The angle theta was scanning from $2\theta=20^\circ$ to $2\theta=70^\circ$ with a step size of 0.02° and a measuring time of 1.25 s per step. The topography and roughness of the films were investigated using an atomic force microscope (DI, Dimension 3100) in contact mode. Hardness and Young's modulus were measured using a load-controlled nano-indentation system (UNI 2000) with a Berkovich indenter. The load dwelling time was 30 s while the indentation depth was 200 nm. Each sample was measured five times, and the average values as well as the deviation were calculated. The corrosion behavior of the films was evaluated by a potetiostat (EG &G 3 273A) coupled to PC, potentiodynamic method in a 0.5 M NaCl solution. The auxiliary and reference electrodes were platinum rod and saturated calomel (SCE) electrode, respectively. The working electrodes sealed with acrylic resin and left an area of $1cm^2$ exposed to the solution during test, were also polarized from -800 mV vs SCE. Open behavior in polarization curves after each experiment the corrosion current (Icorr) and the corrosion potential (Ecorr) were determined using soft core III software.

Table 1 Flow rate of N_2 and Ar and flow ratios of N_2/Ar used for depositing TaN films

Samples	N_2 flow (sccm)	Ar flow (sccm)	N_2/Ar (%)
C_1	5	50	10
C_2	10	50	20
C_3	15	50	30

3 Results and Discussion

Figure 1 shows XRD patterns of samples with different N_2/Ar flow ratios. In all XRD patterns, in addition to the peaks denoted with star are related to 304 stainless steel substrate, peaks of TaN(111), TaN(200) and TaN(220) with FCC structure are observed at $2\theta=35.5^{\circ}$, $2\theta=41.6^{\circ}$ and $2\theta=60.4^{\circ}$, respectively. It can be observed that TaN(111), TaN(200) and TaN(220) peaks intensity in Fig 1 increased with increase of N_2/Ar flow ratio which indicates an improvement in crystalline structure of the films. When the flow ratio of N_2/Ar further increased (sample C_3), TaN(200) and TaN(220) peaks intensity increased, while the TaN(111) peak intensity decreased, which indicates that the preferred orientation of the TaN films have changed.

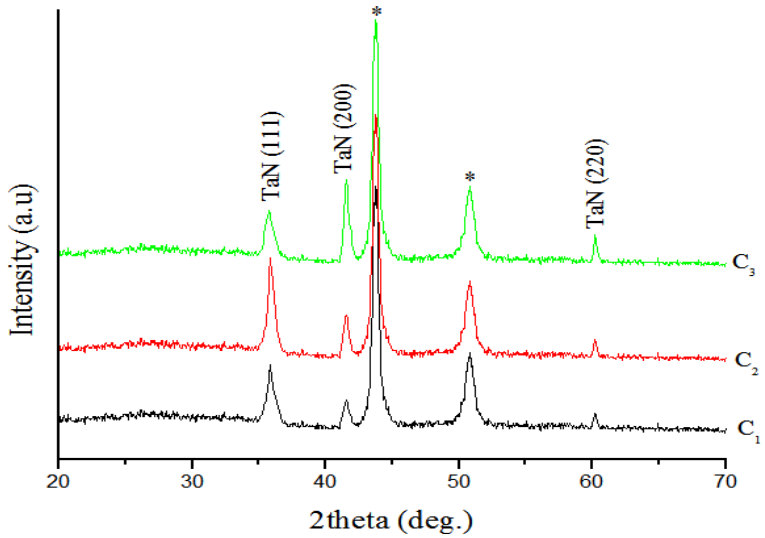

Figure 1. XRD patterns of TaN films prepared at different N_2/Ar flow ratios.

The effect of N_2/Ar flow ratio on the microstructure of different films is shown in figure 2. The surface topography of the films is performed using height AFM for a

scanned area of 2µm×2µm. As observed, the AFM images of samples shows a columnar structure in which the round grains with the nearly equal size are distribution with distance to oneanother on the surface. Table 2 shows the values of average (Ra) and root mean squareroughness (Rms) as well as grain size for samples. The grain size in the AFM images increase as a function of the N_2/Ar flow ratio. Also, the surface roughness of the films increased with the N_2/Ar flow ratio because of the increase of grain size as shown in 2D images of figure2.

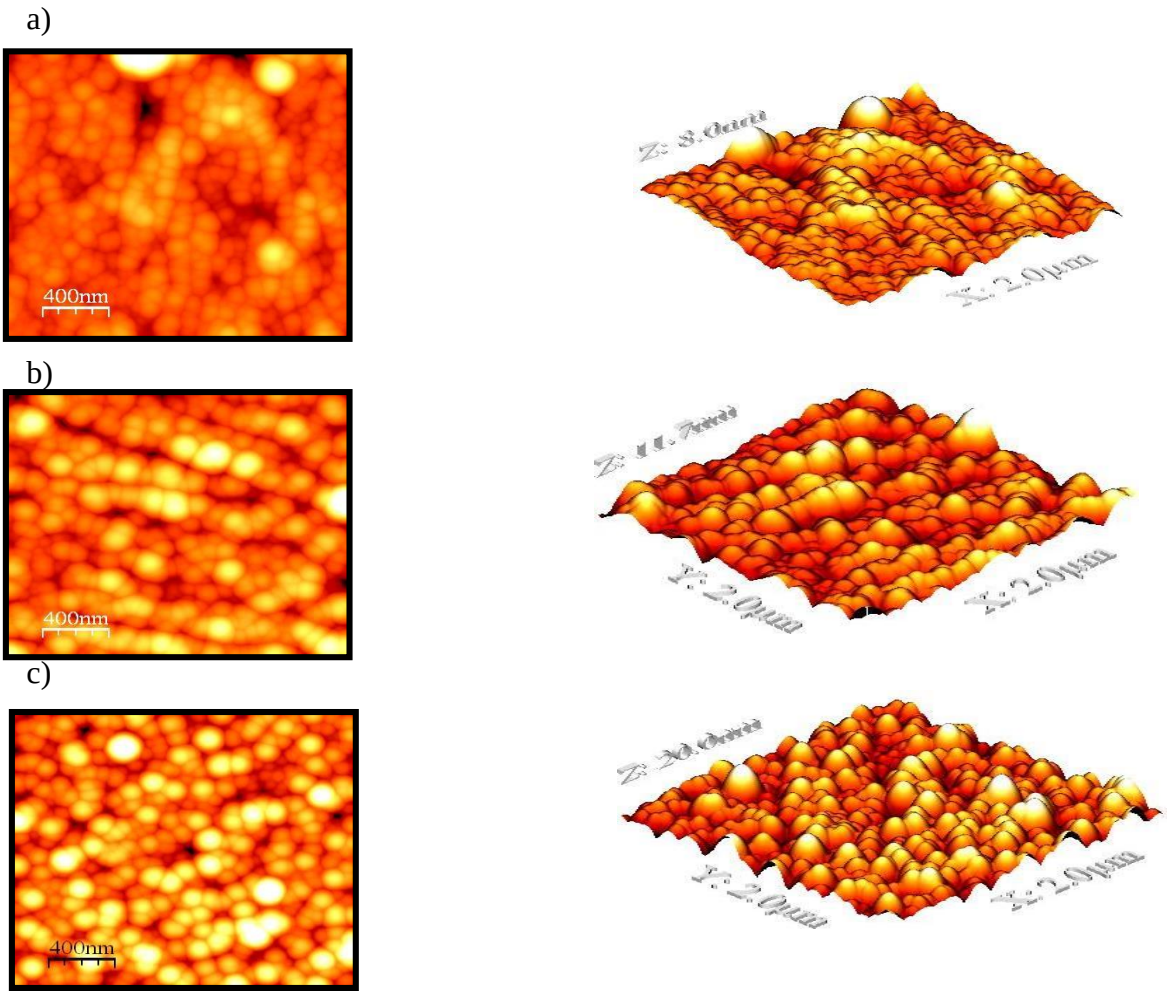

Figure 2. AFM images of TaN films prepared at different N_2/Ar flow ratios: (a) 10%, (b) 20% and (c) 30%.

Table 2 Variation of average roughness and root mean square roughness as well as grain size

Samples	Surface roughness (nm) Rms	Ra	Grain diameter (nm)
C_1	83	61	138
C_2	101	79	146
C_3	161	132	180

Figure 3 shows the hardness and Young's modulus of the films as a function of N_2/Ar flow ratio. The hardness and Young's modulus decreased with the increase of N_2/Ar flow ratio. Overall, factors like surface roughness, N_2/Ar flow ratio and grain size have the greatest impact on hardness and Young's modulus. According to the hardness values obtained in this study, it can be said that grain size has the strongest effect on hardness. Decreasing grain size according to the Hall-Petch equation causes increase in hardness and Young's modulus [15]. The plastic deformation resistance (H^3/E^2) is a strong indicator of a coating's resistance to plastic deformation in the elastic/plastic plate contacts [16]. The high H^3/E^2 of 0.175 was obtained for sample C_1. Hence, it is expected that the sample C_1 show better wear resistance.

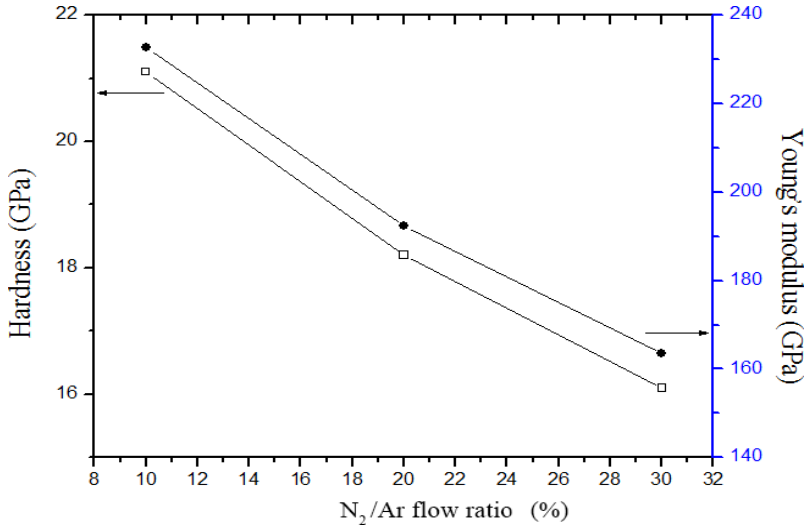

Figure 3. Hardness and Young's modulus of TaN films at different N_2/Ar flow ratios.

The elastic recovery was calculated by the following equation:

$$R= h_{max}-h_r/h_{max} \quad (1)$$

Where h_{max} and h_r are the maximum and residual displacement respectively. Elastic recovery (R) [17], in TaN films were evaluated by load-penetration depth curves of indentations for each film, as show in fig 4. The values decreased from 37% to 28% with increasing of N_2/Ar flow ratio. Potentiodynamic polarization curves of the samples with different N_2/Ar flow ratios are shown in Figure 5.

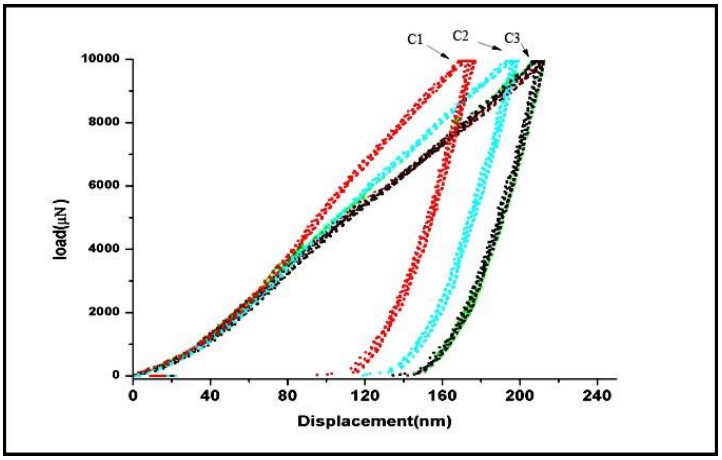

Figure 4. Load-penetration depth curves of indentations for TaN films with different N_2/Ar flow ratios

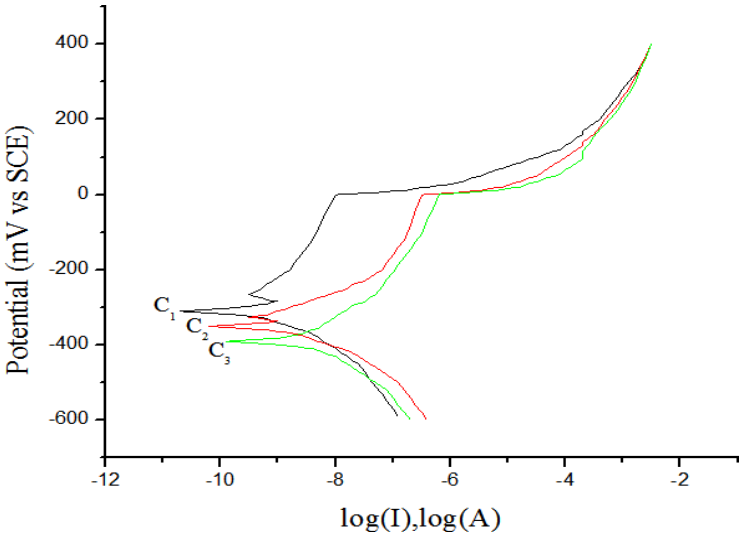

Figure 5. The potentiodynamic polarization curves in 0.5 M NaCl solution for TaN Coatings

The corrosion current and corrosion potential were obtained by the intersection of the extrapolation of anodic and cathodic Tafel curves. The corrosion potential of the different samples as a function of N_2/Ar flow ratio is shown in figure 6. It can be seen with increasing of N_2/Ar flow ratio the corrosion potential increase. According to figure 6 a higher electrochemical stability of films can be observed at sample C_1. Figure 7 shows the corrosion current density (I_{corr}) of samples as a function of N_2/Ar flow ratio. The difference in the corrosive resistivity between different films can be observed from this figure. The I_{corr} increased with increase of N_2/Ar flow ratio and attains a minimal value of 0.035 μA/cm^2 at sample C_1. It is worth noting that the corrosion properties of the films depend greatly on the microstructure of films. As shown in table 2, the grain and surface roughness of films increased with increase of N_2/Ar flow ratio, in result distances between the grains which act as a channel permitting the corrosive electrolyte to penetrate more rapidly down to surface. Overall, the corrosion resistanceis limit mostly by different coating growth defects and other imperfections (open pores, pinholes, voids, micro-cracks), while they act as diffusion paths.

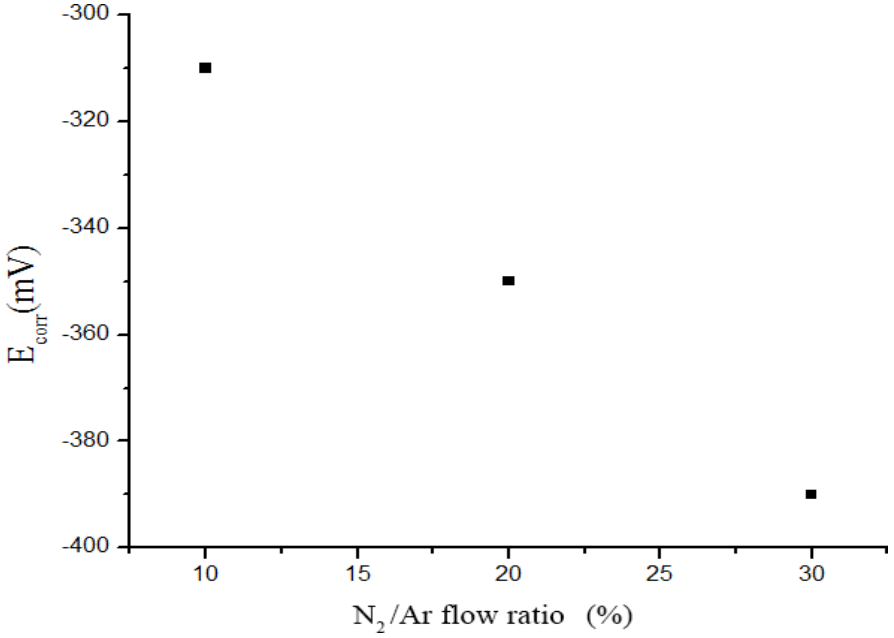

Figure 6. Corrosion potential of the coatings as a function of N_2/Ar flow ratio.

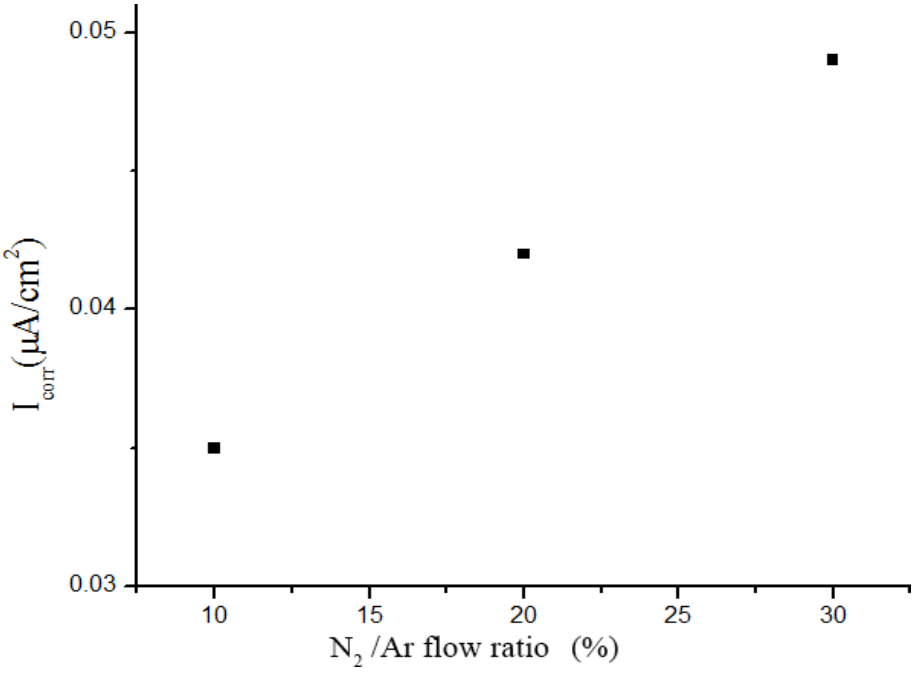

Figure 7. Corrosion current density of the coating as a function of N_2/Ar flow ratio.

4 Conclusions

In the present study, the effect of N_2/Ar flow ratios on the microstructure and mechanical properties of TaN films was investigated. The TaN films with crystalline microstructure features are fabricated by magnetron sputtering with different N_2/Ar flow ratios. XRD patterns showed that TaN crystalline phases were formed into (111), (200) and (220) direction with FCC structure at different N_2/Ar flow ratios. Corresponding to AFM images, grain size and roughness increased with increasing of N_2/Ar flow ratios. A highest hardness and modulus around 21 and 230 GPa respectively, were found for the flow ratio of N_2/Ar =10% due to small grain size and roughness. The minimum corrosion current density of 0.035 μA/cm^2 in 0.5 M NaCl solution in 10% N_2/Ar flow ratio which could be ascribe to the two factors: the structural stuffing and surface roughness decrease.

5 References

[1] M. Kot, W.A. Rakowski, Ł. Major, R. Major, J. Morgiel, J. Surf. Coat. Technol. **202**, 3501 (2008).

[2] D.G. Liu, C.D. Gu, R. Chen, J.P. Tu, J. Surf. Coat. Technol. **205,** 2386 (2010).

[3] M. Sakurai, T. Toihara, M. Wang, W. Kurpsaka, S. Miyake, J. Surf. Coat. Technol. **203**, 171 (2008).

[4] G. Ma, G. Lin, S. Gong, X. Liu, G. Sun, H. Wu, J. Vacuum. **89,** 244 (2013).

[5] H.C. Jiang, C. Wang, W. Zhang, X. Si, Y. Li, J. Mater. Sci. Technol. **26**, 597 (2010).

[6] Y.L. Kuo, J.J. Huang, S.T. Lin, C. Lee, W.H. Lee, J. Mater. Chem. Phys. **80**, 690 (2003).

[7] Q. Xie, J. Musschoot, C. Detavernier, D. Deduytsche, R.L.V. Meirhaeghe, S.V. denBerghe, Y.L. Jiang, G.P. Ru, B.Z. Li, X.P. Qu, J. Microelectron. Eng. **85**, 2059 (2008).

[8] Y.K. Lee, K.M. Latt, K. Jaehyung, K. Lee, J. Mater. Sci. Semicond. Process. **3**, 179 (2000).

[9] S.R. Burgess, H. Donohue, K. Buchanan, N. Rimmer, P. Rich, J. Microelectron. Eng. **64**, 307 (2002).

[10] S.K. Kim, B.C. Cha, J. Thin Solid Films. **475**, 202 (2005).

[11] Y.X. Leng, H. Sun, P. Yang, J.Y. Chen, J. Wang, G.J. Wan, N. Huang, X.B. Tian, L.P. Wang, P.K. Chu, J. Thin Solid Films. **471**, 398–399 (2001).

[12] C.S. Shin, Y.W. Kim, D. Gall, J.E. Greene, I. Petrov, J. Thin Solid Films. **402**, 172 (2002).

[13] G.R. Lee, H. Kim, H.S. Choi, J.J. Lee, J. Surf. Coat. Technol. **201**, 5207 (2007).

[14] Y. Kang, C. Lee, J. Lee, J. Mater. Sci. Eng. B. **75**, 17 (2000).

[15] W.L. Li, W.D. Fei, Y. Sun, J. Mater. Sci. Lett. **21**, 239-241 (2002).

[16] T.Y. Tsui, G.M. Pharr, W.C. Oliver, C.S. Bhatia, R.L. White, S. Anders, A. Anders, I.G. Brown, J. Mater. Res. Soc. Symp. Proc. **383**, 447 (1996).

[17] A. Leyland, A. Matthews, J. Wear. **246**, 1-11 (2000)